N94-31031

# MORPHOLOGY CORRELATION OF CRATERS FORMED BY HYPERVELOCITY IMPACTS

Gary D. Crawford
Mechanical Engineering Department
Auburn University, AL 36849
Phone: 205/844-4822

M. Frank Rose
Space Power Institute
Auburn University, AL 36849
Phone: 205/844-5894

Ralph H. Zee
Mechanical Engineering Department
Auburn University, AL 36849
Phone: 205/844-4822

## SUMMARY

Dust-sized olivine particles were fired at a copper plate using the Space Power Institute hypervelocity facility, simulating micrometeoroid damage from natural debris to spacecraft in low-Earth orbit (LEO). Techniques were developed for measuring crater volume, particle volume, and particle velocity, with the particle velocities ranging from 5.6 to 8.7 km/s. A roughly linear correlation was found between crater volume and particle energy which suggested that micrometeoroids follow standard hypervelocity relationships. The residual debris analysis showed that for olivine impacts of up to 8.7 km/s, particle residue is found in the crater. By using the Space Power Institute hypervelocity facility, micrometeoroid damage to satellites can be accurately modeled.

## INTRODUCTION

The Long Duration Exposure Facility (LDEF) was in LEO for 5 years and 9 months. It was designed to study the space environment and to investigate the effects of this environment on space operations. Upon retrieval of LDEF, NASA personnel of the Meteoroid and Debris Special Investigation Group (M&D SIG) identified a total of approximately 34,000 features caused by micrometeoroid impacts (ref. 1). These results offer staunch proof for the need to successfully model the effects of micrometeoroid impacts on future space missions. While it is unlikely that micrometeoroids could cause catastrophic structural damage to a spacecraft, they can cause extensive damage to windows, solar cells, protective coatings, and other more delicate components.

Micrometeoroids are dust-sized particles in space, and they can be divided into two groups: interplanetary and orbital. As their names imply, the orbital micrometeoroids are in orbit around the Earth, and the interplanetary micrometeoroids come from space. The most important difference between

them is their average collision velocities. For two objects in LEO, their average collision velocity is around 10 km/s. An interplanetary micrometeoroid will impact with an object in LEO at a velocity of 15 to 20 km/s (ref. 2). In order to properly model LEO impacts, a velocity range from 5 to 20 km/s must be examined. The term "hypervelocity" is used to describe objects traveling at these speeds.

The chemical composition of micrometeoroids varies depending on their origin, which is either natural or man-made. Natural micrometeoroids are composed of metallic mixtures of elements such as iron, magnesium, silicon, aluminum, calcium, and/or sulfur (ref. 3). The relative amounts of each element vary. The man-made micrometeoroids, as their name implies, are a result of debris placed in space by man. Their chemical composition varies widely. For example, a window on one of the space shuttles had to be replaced due to an impact by what was thought to be a paint chip (ref. 4).

Therefore, in order to simulate hypervelocity impacts of micrometeoroids, care must be taken in choosing proper particle velocities and composition.

## OBJECTIVE

There are three main objectives to this research: (1) verify the ability of the Auburn University Space Power Institute hypervelocity impact facility to simulate micrometeoroid collision phenomena; (2) develop a procedure for analyzing hypervelocity impact experiments at the Space Power Institute; and (3) examine the correlation between various crater and impacting particle parameters for micrometeoroid impacts. The facility is already being used to simulate micrometeoroid impacts, and this research is designed to help improve the techniques for material analysis. This kind of information can be used to duplicate micrometeoroid phenomena on LDEF, or test how well future materials can survive the orbital environment.

## Hypervelocity Simulation

The Space Power Institute at Auburn University has a unique hypervelocity simulation system. The hypervelocity impact facility (HIF) accelerates microgram size particles to speeds in excess of 5 km/s. Velocities of 8 to 10 km/s are reached on a regular basis, and velocities of around 15 km/s have been attained. The HIF accelerates the particles using a mixture of electromagnetic acceleration, thermal expansion, and plasma drag. The firing environment is fully enclosed, and a vacuum is held which is comparable to that of space.

In general, hypervelocity impacts follow the relationship of equation

$$V = K^{*}E \tag{1}$$

where $V$ is the volume of the crater, $E$ is the kinetic energy of the particle, and $K$ is a proportionality constant (ref. 5). In order to verify this relationship, the mass and velocity of the incoming particle must be known, along with the volume of the resulting crater.

The velocity of the impacting particle that causes each crater is found using streak photography methods (Figure 1). The streak camera looks across the surface of the target plate, so each impact is registered as a bright flash on the camera film. The camera is also set up to view the target plate from two directions which are 90° from each other, thus providing an X-axis and a Y-axis view of the impact.

The resulting streak photograph is shown at the bottom half of Figure 1. The photograph tells the time at which a particular impact occurred, and because each impact is viewed from two directions, the location of the impact on the plate can be found. By knowing the time of impact for a particular crater, and by knowing the distance of the flight tube, the velocity of the impacting particle is calculated (ref. 6).

A thin Mylar™ film of about 1 micron is placed an inch above the target plate. The particles must pass through this Mylar™ before impacting. Although some of the particles break up upon hitting the Mylar™, most are of sufficient size (50 to 100 microns in diameter, or more) to remain intact. Immediately after a launch, the target plate (with its Mylar™ still in position above the plate) is taken to a specially designed optical inspection device. Here, the cross-sectional area of the impacting particle is measured, and this is compared to earlier particle size measurements.

## Experimental Procedure

The procedure developed for this research can be divided into five main steps:

1. Choose the target and particle materials
2. Conduct the hypervelocity simulation, gathering velocity and size information
3. Use the energy-dispersive spectrometer (EDS) of the scanning electron microscope (SEM) to check for particle residue
4. Use the confocal scanning laser microscope (CSLM) and the planar morphometry digitizer (PMD) to measure crater volume
5. Correlate the above information to describe the hypervelocity impact phenomena.

A cold-rolled annealed copper plate was used for a target plate. Copper was chosen for reasons of chemical analysis. The EDS of the SEM tells the presence and relative amounts of elements on a material's surface, but it does not tell the chemical structure. When the HIF launches the particles, a certain amount of debris is carried down the launch tube along with the particles. This debris is composed of several different elements, but copper is not one of them. The residual debris from an impacting particle is much easier to distinguish against the copper material background. Another reason for using copper was because it is a conductor of electricity and this gives better imagery on the SEM.

Olivine was chosen as the particle material. This substance is a metallic mixture of mainly magnesium, silicon, and iron. Olivine was used because several of the craters on LDEF had olivine residue in them (ref. 7), and the magnesium in the olivine distinguishes it from other hypervelocity debris produced by the HIF launching process. The particles were spheroidized by a private contractor prior to firing, so they would have a relative uniform shape. Figures 2 and 3 show the olivine spheres. The spheres were between 40 and 70 micrometers in diameter, and a preliminary EDS analysis of the olivine was made before firing. Note the different particle morphologies shown in Figure 3. Even though the particles looked different, they had the same elemental compositions. The different particle textures may have caused some of the different crater morphologies.

A CSLM and a PMD were used to measure the volume of the craters. The CSLM is unique in that it has a small depth of field, and areas which are not in focus are not visible (ref. 8). The result is photographs which show "slices" of a crater (Figure 4). These "slices" are cross sections of a crater at

various elevations above the bottom of the crater. The area of the cross sections was found using the PMD. By taking slices at various heights above the crater bottom, a direct calculation of the crater volume was made. Between 12 and 15 slices were taken of each crater, up to the original material surface (this was done on all the craters for uniformity). The CSLM also produces a profile of the crater, as shown in Figure 5. This side view was used to check the crater depth and diameter.

One of the problems with the CSLM was the reflectivity of the material surface, and this is the reason for much of the "fuzziness" in the pictures. This was partially compensated for by coating the copper surface with carbon, which had the added effect of making the craters easier to photograph on the SEM. The coating seemed to be less effective on the smaller crater, but accurate measurements were still made by making comparisons with some of the clearer CSLM photos.

## Data Analysis

Table 1 shows the characteristics of the craters that were analyzed, and Table 2 shows relevant information about the particles that caused the craters. The tables list the data from highest to lowest particle velocities.

The crater diameter to crater depth relationship shown in Table 1 is between 2 and 2.6, which is typical for hypervelocity impacts into a copper plate (ref. 9). The crater volume calculations are of particular interest. The measured crater volume values were obtained from the CSLM measurements, and the calculated values came from using the equation for the volume of a sphere. Some of the calculations are almost equal to the measurements, while others differ by a factor of 2. On average, the calculated volume was around 28 percent larger than the measured volume.

The particle mass, given in Table 2, was calculated by multiplying the density of the olivine by the volume of the particle. As shown in Figures 2 and 3, the olivine was approximately spherical. The radius of a given particle was found from the area of the hole in the Mylar™ (which was roughly spherical), and the volume was calculated using the equation for a sphere. The particle energy is simply the kinetic energy of the particle.

From the tables, a plot of crater volume versus particle energy was made. This is Figure 6, and the plot shows the linear relationship described earlier in this report. Thus, the characteristic hypervelocity relationships were attained by the HIF.

There are several areas for error in the data collection, and these areas were probably what caused the scattering of the data. The olivine particles were assumed to have uniform density, but the spheroidization process may have varied their densities some. The Mylar™ film is susceptible to a certain amount of shrinking and expanding due to the environmental temperatures. Ejecta from the craters causes holes in the Mylar™, and some of these holes may have been mistaken as being caused by particles. As many as 40 to 100 particles may impact on a 12-$cm^2$ target plate in one simulation, which makes the streak record difficult to read. Several craters were not used in the analysis because the streak data did not match. (This problem has now been solved by decreasing the number of particles striking the target.)

## Photographic Analysis

Figures 7 through 10 show two of the craters. Figures 7 and 8 were formed by the particle moving 8.7 km/s, and Figures 9 and 10 were formed by the particle moving 8.1 km/s. Even though these are two of the faster impacts, their shape and characteristics were endemic to all the craters.

Figure 7 is an overhead view of the crater. Note the distinctive lip all around the crater, and the number of nearby smaller craters. The smaller craters were probably caused by particle breakup as it went through the Mylar™. The inside of the crater is coated with olivine particle residue, which is very similar to many of the craters analyzed on LDEF (ref. 10). The residue is thick on the side of the crater, and appears thinner in the bottom of the crater. This is shown better in Figure 8. On the right edge of the photo some porosity is visible, and the light gray area is the exposed copper surface at the bottom of the crater. The surrounding dark gray region is olivine residue from the impacting particle.

The crater in Figure 9 is also an olivine crater, and had a practically identical EDS analysis. Yet there is a very different morphology. Olivine residue was found throughout the interior of the crater, although there appears to be less residue on the crater lips than was on the previous crater. Figure 10 shows the morphology in the crater base. It had the same material composition as the previous crater, but a very different texture. There appears to be no thinning of residue in the bottom of the crater. Most of the residue appears to have melted (i.e., it has a smooth surface), but some of the residue shows a racked, granular structure associated with a brittle fracture (ref. 11).

One of the most important features of both craters is the lack of gun debris in the craters. In those craters that are thought to have been caused by gun debris, particle residue was found along the lips of the crater. This residue was composed of as many as 10 different elements from various parts of the gun. There was no such residue around or in the olivine craters, thus showing there was no mixing of olivine and gun debris.

## CONCLUSIONS

The Space Power Institute HIF accurately models space micrometeoroid phenomena. For olivine-like substances, a certain number of particles will arrive at the target intact. There will be some gun debris and some particle disfigurement, but accurate impact simulations can be made.

By reproducing known hypervelocity relationships, it has been shown that the methods for finding the various particle and crater parameters are reasonably accurate. The HIF can be used to test materials' parameters, so engineers can characterize the best materials to survive the micrometeoroid environment.

Olivine impacts into a copper plate leave particle residue in the crater for velocities of up to at least 9 km/s. The analysis so far suggests that there is a velocity at which no olivine would be left in the crater, and this research is currently being continued at the HIF. Once this upper limit has been established, comparisons can be made with craters on retrieved satellites to provide an additional method for measuring micrometeoroid impact velocities encountered in space.

## ACKNOWLEDGMENTS

This research was partially supported by NASA Marshall Space Flight Center and NASA Langley Research Center. Mr. Steve Best of the Space Power Institute at Auburn University is head engineer of the Hypervelocity Impact Facility, and was exceptionally helpful. Dr. Wartan A. Jemian gave advice for using the planar morphometry digitizer, and Dr. Roy Wilcox aided in the scanning electron microscopy evaluations of the materials. Dr. David Hill of the Space Power Institute lent his

expertise of hypervelocity phenomena. The confocal scanning laser microscope that was used for this work is located at the Center for Ultrastructural Studies at the University of Georgia at Athens, and is under the care of Dr. Mark Farmer. Dr. Farmer provided the instruction for its use.

## REFERENCES

1. See, T., Allbrooks, M., Atkinson, D., Simon, C., and Zolensky, M.: "Meteoroid and Debris Impact Features Documented on the Long Duration Exposure Facility: A Preliminary Report." NASA JSC No. 24608, August 1990, pp. 59.

2. Kessler, D.J.: "Current Orbital Debris Environment." In *Orbital Debris From Upper-Stage Breakup*, J.P. Loftus, Jr., editor, Progress in Astronautics and Aeronautics, vol. 121, AIAA 89-36977, 1989, pp. 3–5.

3. Horz, F., Bernhard, R.P., Warren, J., See, T.H., Brownlee, D.E., Laurance, M.R., Messenger, S., and Peterson, R.B.: "Preliminary Analysis of LDEF Instrument A0187–1, Chemistry of Micrometeoroids Experiment." In *LDEF—69 Months in Space*, A.S. Levine, editor, NASA CP-3134, June 2–8, 1991, pp. 487–498.

4. Kessler, D.J.: "Current Orbital Debris Environment." In *Orbital Debris From Upper-Stage Breakup*, J.P. Loftus, Jr., editor, Progress in Astronautics and Aeronautics, vol. 121, AIAA 89–36977, 1989, p. 9.

5. Zukas, J.A., Nicholas, T., Swift, H.F., Greszczuk, L.G., and Curran, D.R.: "Impact Dynamics." John Wiley and Sons, Inc., 1982, pp. 216–218.

6. Rose, M.F., and Best, S.: "HYPER: Auburn University's Hypervelocity Impact Facility." Space Power Institute, Auburn University, 1992.

7. Horz, F., and Bernhard, R.P.: "Compositional Analysis and Classification of Projectile Residues in LDEF Impact Craters." NASA TM-104750, June 1992.

8. Kino, G.S., and Corle, T.R.: "Confocal Scanning Optical Microscopy." Physics Today, vol. 42, September 1989, pp. 55–61.

9. Herrman, W., and Wilbeck, J.S.: "Review of Hypervelocity Impact Theories." Int. J. Impact Engng., vol. 5, 1987, pp. 307–310.

10. Horz, F., and Bernhard, R.P.: "Compositional Analysis and Classification of Projectile Residues in LDEF Impact Craters." NASA TM-104750, June 1992.

11. Askeland, D.R.: "The Science and Engineering of Materials." PWS Publishers, Wadsworth, Inc., 1984, pp. 711–725.

Table 1. Crater data.

| Particle Velocity (km/s) | Crater Diameter (μm) | Crater Depth (μm) | Crater Diameter/ Depth | Measured Crater Volume (1,000 μm$^3$) | Calculated Crater Volume (1,000 μm$^3$) | Percent Difference From Measured Volume |
|---|---|---|---|---|---|---|
| 8.7 | 203 | 100 | 2 | 1,089 | 2,094 | 92 |
| 8.3 | 185 | 88 | 2.1 | 1,297 | 1,539 | 19 |
| 8.1 | 100 | 51 | 2 | 151 | 261 | 73 |
| 7.8 | 250 | 111 | 2.3 | 3,175 | 3,441 | 8 |
| 7.3 | 196 | 77 | 2.6 | 1,061 | 1,403 | 32 |
| 6.6 | 165 | 70 | 2.4 | 713 | 928 | 30 |
| 6.1 | 183 | 73 | 2.5 | 965 | 1,165 | 21 |
| 6 | 151 | 61 | 2.5 | 567 | 665 | 17 |
| 5.8 | 132 | 59 | 2.2 | 468 | 511 | 9 |
| 5.7 | 145 | 63 | 2.3 | 643 | 651 | 1 |
| 5.7 | 136 | 57 | 2.4 | 563 | 511 | 9 |
| 5.6 | 220 | 90 | 2.4 | 1,931 | 2,094 | 8 |
| 5.6 | 200 | 95 | 2.1 | 1,250 | 1,941 | 55 |

Table 2. Particle data.

| Particle Velocity (km/s) | Particle Diameter (μm) | Particle Mass (μgram) | Particle Energy (joules) | Particle Energy per Unit Mass (j/μgram) |
|---|---|---|---|---|
| 8.7 | 53 | 0.25 | 9.4 | 37.6 |
| 8.3 | 45 | 0.15 | 5.2 | 34.7 |
| 8.1 | 36 | 0.08 | 2.5 | 31.3 |
| 7.8 | 77 | 0.78 | 23.6 | 30.3 |
| 7.3 | 64 | 0.44 | 11.7 | 26.6 |
| 6.6 | 54 | 0.27 | 5.9 | 21.9 |
| 6.1 | 42 | 0.12 | 2.3 | 19.2 |
| 6 | 60 | 0.36 | 6.5 | 18.1 |
| 5.8 | 45 | 0.15 | 2.5 | 16.7 |
| 5.7 | 33 | 0.06 | 1 | 16.7 |
| 5.7 | 29 | 0.04 | 0.6 | 15.0 |
| 5.6 | 67 | 0.51 | 8 | 15.7 |
| 5.6 | 71 | 0.6 | 9.4 | 15.7 |

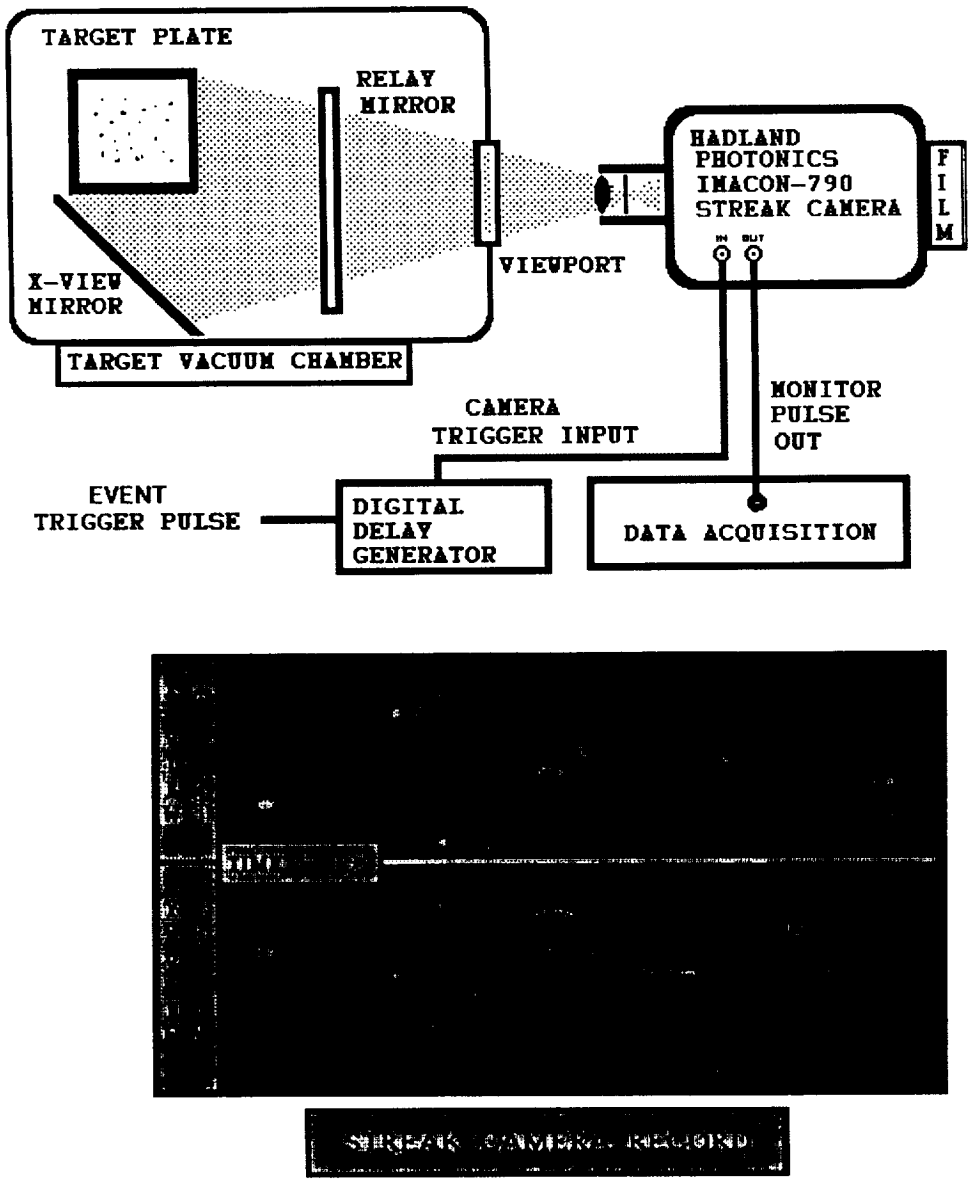


Figure 1. Streak photography diagram.

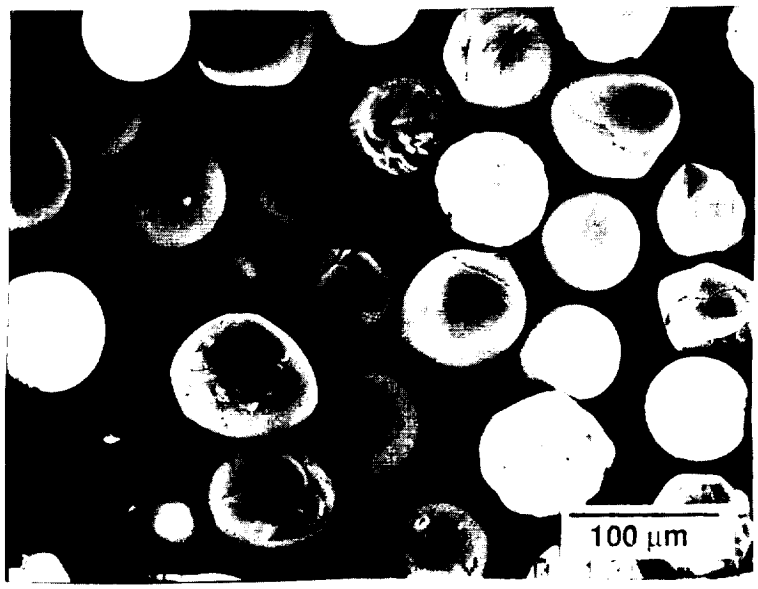


Figure 2. Spheroidized olivine particles that were used in this experiment. Their diameters ranged from 40 to 100 micrometers (× 200).

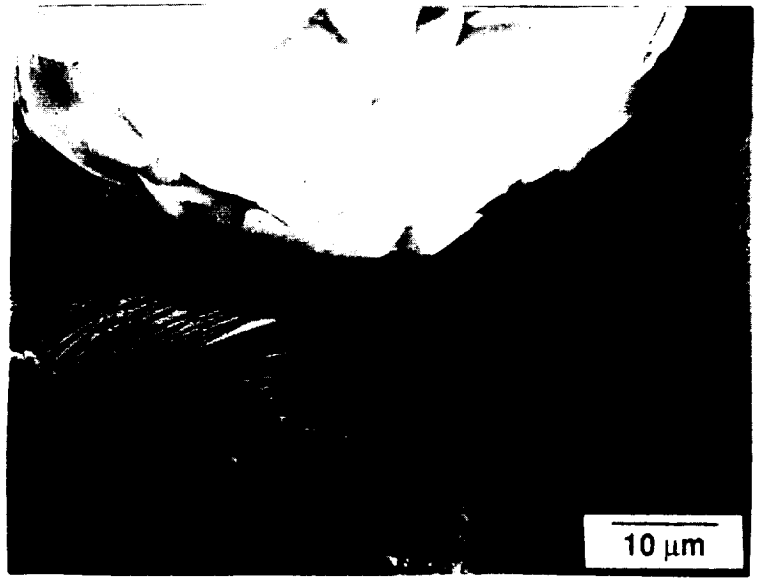


Figure 3. Closeup view of the olivine particles showing the different morphologies (× 1,500).

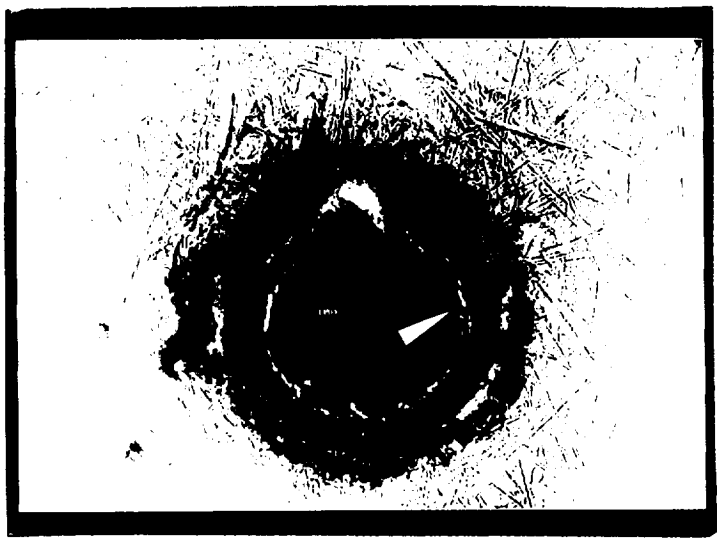

Figure 4. CSLM overhead cross section of a crater formed by a 5.6-km/s particle. The elevation of the cross section above the crater bottom is 100 micrometers, and the white arrow shows the outline of the crater. Note how the irregular shape of the crater is shown.

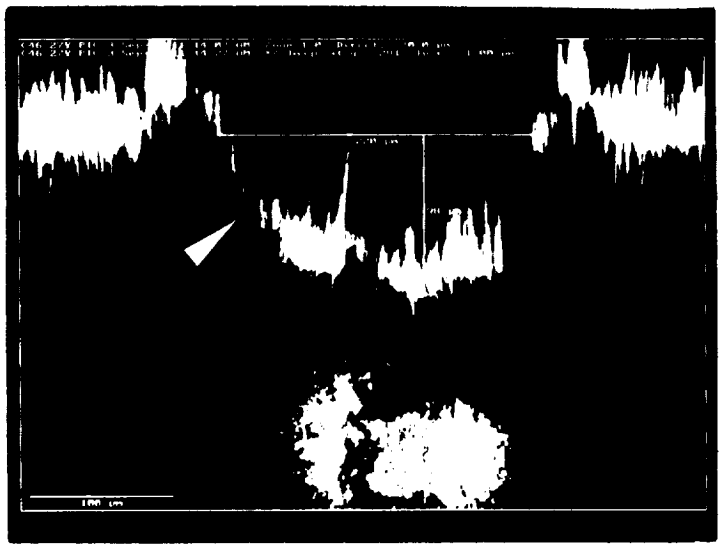

Figure 5. CSLM side cross section of the same crater shown in Figure 4. The white arrow points to the crater surface. Note that the crater depth is measured from the original material surface.

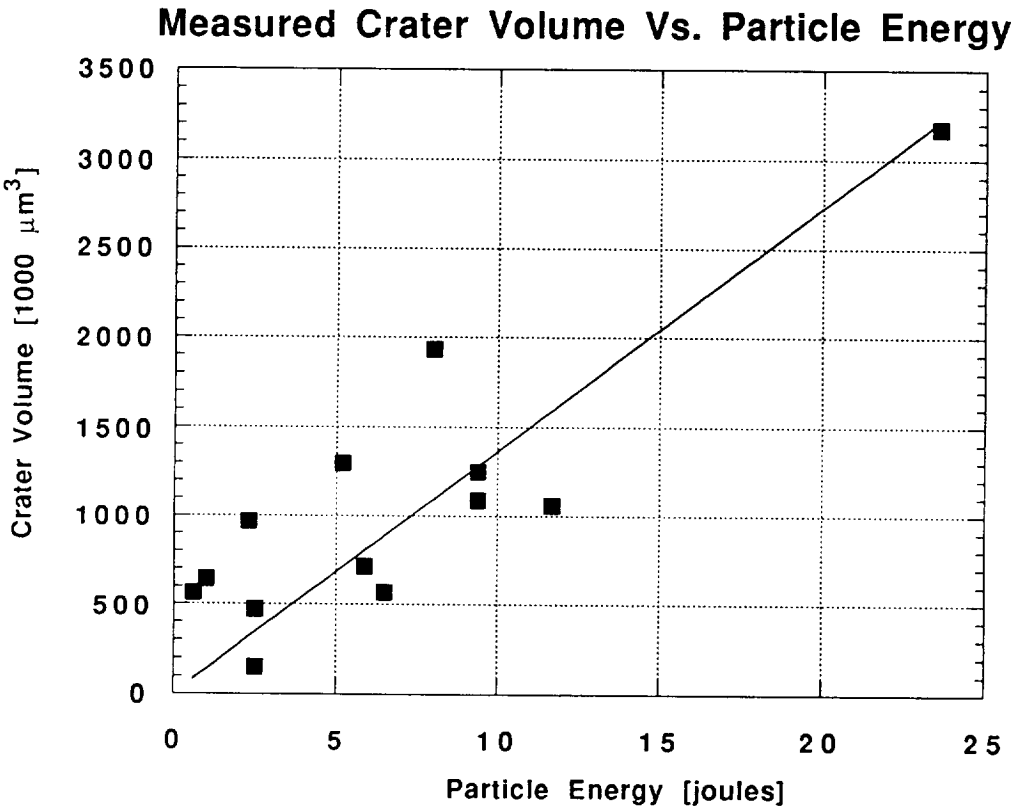


Figure 6. Measured crater volume versus particle kinetic energy. Note the linear correlation, as described in equation (1).

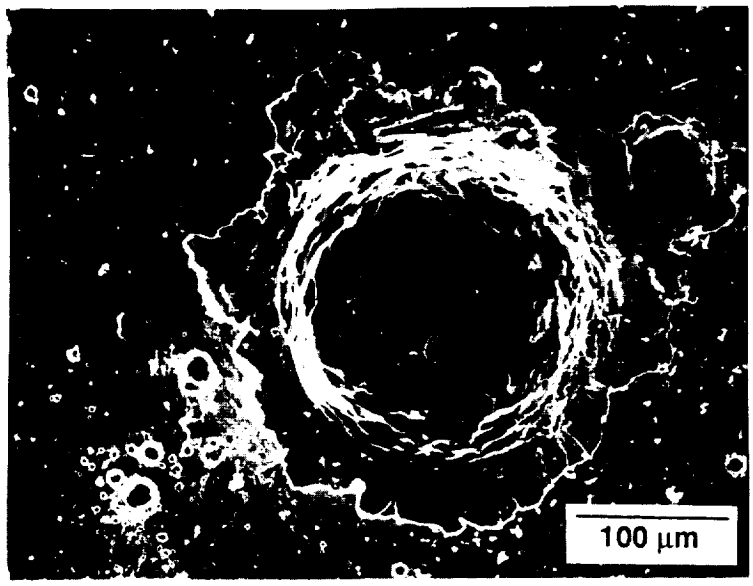


Figure 7. Crater formed by an olivine particle moving 8.7 km/s. Note smaller craters formed by minor particle breakup (× 200).

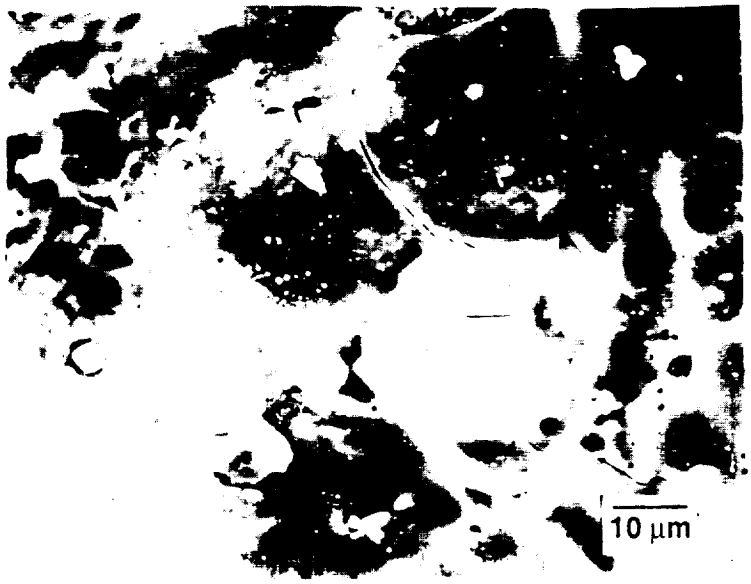


Figure 8. Interior of crater shown in Figure 7. The light colored area to the right of center is the exposed target surface. Note the porosity on the right (× 1,000).

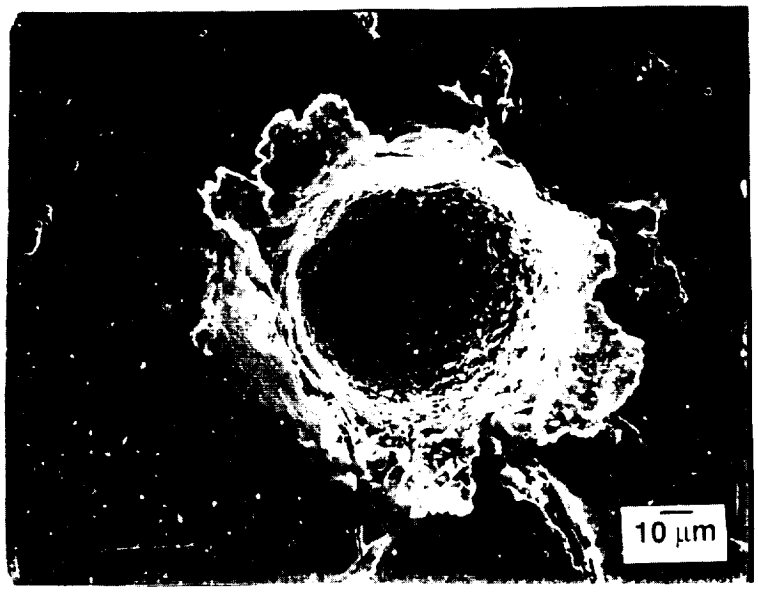


Figure 9. Crater formed by an olivine particle moving 8.1 km/s. The residue has the same EDS scan as the crater in Figure 7 (× 400).

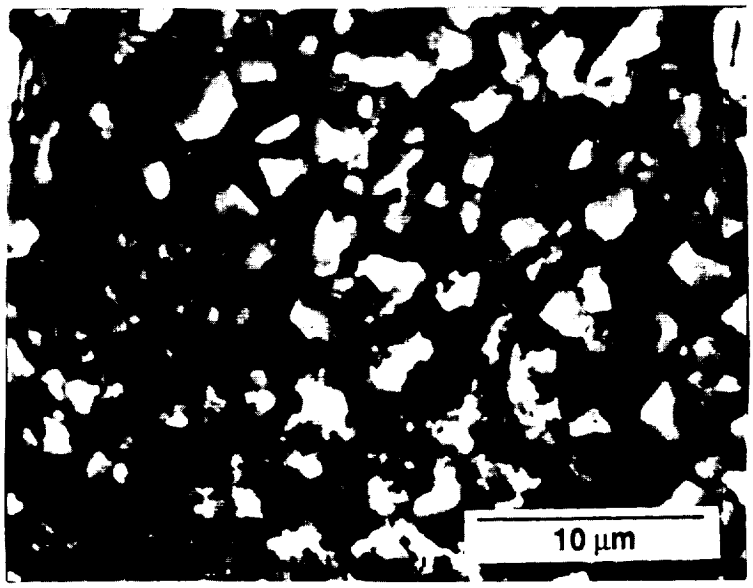


Figure 10. Interior of the crater shown in Figure 9. Compare to the morphology of Figure 8. Note the melted material underneath the jagged grains (× 3,000).